Hydrogen Bonding in Fluorinated Amides: FTIR, Two Dimensional Correlation Spectroscopy and DFT Calculations

Stefano Radice,[*1] *Alberto Milani,*[2] *Chiara Castiglioni*[2]

Summary: Fluorinated macromers with amidic functional groups are used as additives in several high tech applications. We show here how aggregation phenomena related to hydrogen bonding are one of the key factor determining their chemical/physical and macroscopic properties. IR spectra are analyzed depending on different external parameters such as the concentration of amide groups and temperature. The experimental findings have been interpreted by means of DFT (Density Functional Theory) calculations on suitable molecular models. Moreover, 2D correlation spectroscopy has been applied to different sets of data, considering concentration and temperature as perturbing variables. The two dimensional correlation approaches confirmed the computational results and give an overall interpretation of the effects due to concentration and temperature.

Keywords: first principles calculations; fluorinated amides; FTIR spectroscopy; two dimensional correlation spectroscopy

Introduction

Fluorinated materials based on a perfluoropolyalkyl-ether chain backbone (PFPE) are widely used in high tech applications due to their excellent chemical, thermal and mechanical performance properties. Inside this class of polymeric materials, end groups and chemical building blocks may be tailored according to specific needs; recently we studied association properties of PFPE with carboxylic acid end groups[1]. For specific purposes[2] fluorinated macromers with amidic functional end groups have been produced and used in demanding lubrication applications[3]. IR spectroscopy measurements and molecular modeling of these fluorinated amides have been carried out in order to obtain a molecular characterization of the chemical/physical phenomena ruling their macroscopic properties, such as aggregation via hydrogen bonding. The aim of this study is to characterize the intermolecular interactions taking place in different solutions due to the occurrence of hydrogen bonding and to understand how key parameters such as the concentration of amide groups and the temperature play a role on the molecular aggregation of these systems.

Experimental and Computational Details

In Ref. [4] the spectroscopic features of amide macromers of formula $CF_3O[CF_2CF(CF_3)O]_p[CF_2O]_qCF_2C(O)NH_2$ have been studied considering solution of the following fluorinated polymer matrix: FOMBLIN® M03, GALDEN® D02 and HGALDEN® ZV60. In this contribution, we focus on FOMBLIN® M03 [formula CF_3-O-(CF_2-CF_2-O)$_p$-(CF_2-O)$_q$-CF_3] solutions and we analyze in detail the thermal evolution of the IR spectra.

[1] Solvay Solexis, Research & Technology, Viale Lombardia 20, Bollate (MI), 20021, Italy
E-mail: stefano.radice@solvay.com
[2] Politecnico di Milano, Dip. Chimica, Materiali, Ing. Chimica ''G. Natta'', Piazza Leonardo da Vinci, Milano, 20100, Italy

IR spectra were recorded with a Thermo Nicolet Nexus® 870. Acquisition parameters: 256 scans with a resolution of $2\,cm^{-1}$. The samples were kept in suitable liquid cell with 1mm fixed optical pathlength. For experiments while varying temperature we used the Variable Temperature cell by Specac, recording both sample and empty cell spectra for each temperature (in order to have the best signal to noise ratio to perform spectral subtractions).

Density Functional Theory (DFT) calculations have been carried out by using Gaussian 03 package[5], adopting the B3LYP hybrid exchange-correlation functional[6–7] and 6–311 + +G** basis set.

The molecular model adopted for the modeling has the chemical formula CF_3-CF_2-CF_2-CF_2-$CONH_2$: in addition to the calculation on the isolated molecule, in Ref. [4] a wide investigation of the possible hydrogen bonding dimers and trimers was carried out. In particular, in the next analysis, in addition to the isolated molecule, the two dimers sketched in Figure 1 will be considered for the interpretation of temperature dependent IR spectra.

The selection of these two dimers only is dictated by the fact that the main features observed in the experimental spectra can be directly explained based on the contribution of the isolated molecule and of these dimers while the other complexes are responsible only for minor features, as indicated in Ref. [4]. Furthermore, the models here adopted do not contain the oxygen atoms of the ether group, contrary to the experimental sample: test calculations have been carried out on models which reproduces the chemical structure of the real polymer and negligible differences have been found in the NH stretching bands. Therefore, the model here adopted is more general and can be transferred to the interpretation of similar molecules, thus giving an interpretation of hydrogen bonding effects in perfluorinated amides on a general ground.

Results and Discussion

IR Spectra and DFT Calculations

In Figure 2 the experimental IR spectra of FOMBLIN® M03 solutions are reported for increasing concentration (weigth/weight, left panel) of the fluorinated amide or for increasing temperature (right panel). The 3600–3400 cm^{-1} range is shown in Figure 2, namely the region where generally the ''free'' (not involved in hydrogen bonding) NH stretching bands are observed.

On the basis of these spectra two main observations can be done: first, the overall pattern is quite complex, and it is possible to identify at least three bands associated to ''free'' NH stretching at 3560 cm^{-1}, 3512 cm^{-1} and 3438 cm^{-1}; notice that in the case of a molecule not involved in hydrogen bonding only two bands are expected in this region (two NH bonds are indeed present). Second, the spectra show a peculiar evolution with concentration and temperature and in particular the bands at 3512 cm^{-1} gains intensity when

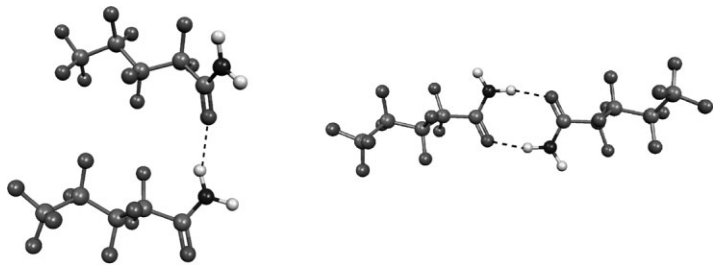

Figure 1.
Sketch of the model hydrogen-bonded dimers used in DFT calculations. Left: Dimer 1HB (one hydrogen bond); Right: Dimer 2HB (Two hydrogen bonds).

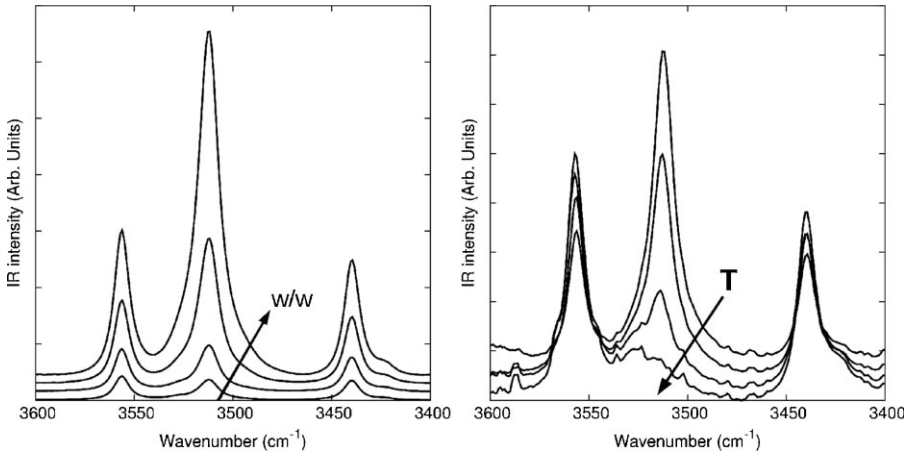

Figure 2.
Experimental IR spectra of FOMBLIN® M03 solutions (spectral subtraction of fluorinated matrix has been done) at increasing concentrations (left) or increasing temperature (right). The arrows indicate the direction of increasing concentration/temperature.

increasing the concentration or decreasing the temperature.

In order to rationalize these observations, IR spectra have been calculated for the isolated molecule and hydrogen bonded dimers and the results are reported in Table 1. In the case of the isolated molecule two bands are indeed found and are associated with the symmetric and antisymmetric NH stretching involving the $-NH_2$ group. In the case of dimers a peculiar behaviour is predicted: a stretching vibration mainly localized on the NH bond directly involved in hydrogen bonding as donor is found at much lower wavenumbers and shows a large value of intensity, following the well-known[8] spectral behaviour expected when hydrogen bond occurs. Furthermore, this finding can be immediately correlated to the large and broad band which is observed in the experimental spectra in the range 3400–3100 cm^{-1} (shown in Figure 3).

However, due to the presence of $-NH_2$ groups, in both the hydrogen bonded dimers sketched in Figure 1 also NH bonds not directly involved in H bond are still present. In these cases, the occurrence of

Table 1.
Assignment of the experimental IR bands based on the computed values (B3LYP/6-311++G**) of NH stretching frequencies (cm^{-1}) and IR intensities (km/mol) for the isolated molecule and H-bonded dimers. For a better comparison with the experimental spectra, the DFT computed frequency values have been scaled by a 0.957 factor, determined by the fitting of the experimental spectra.

	Frequency [DFT] (cm^{-1})	IR intensity [DFT] (km/mol)	Frequency [Experim.] (cm^{-1})
Dimer 2HB	3178	0	//
	3218	1699	3247 (broad)
Dimer 1HB	3394	322	3350 (broad)
Dimer 1HB	3430	76	3423 (shoulder)
Isolated	3435	71	3438
Dimer 2HB	3511	314	3512
	3511	1	//
Dimer 1HB	3524	158	3527 (shoulder)
Dimer 1HB	3553	88	3545 (shoulder)
Isolated	3560	83	3560

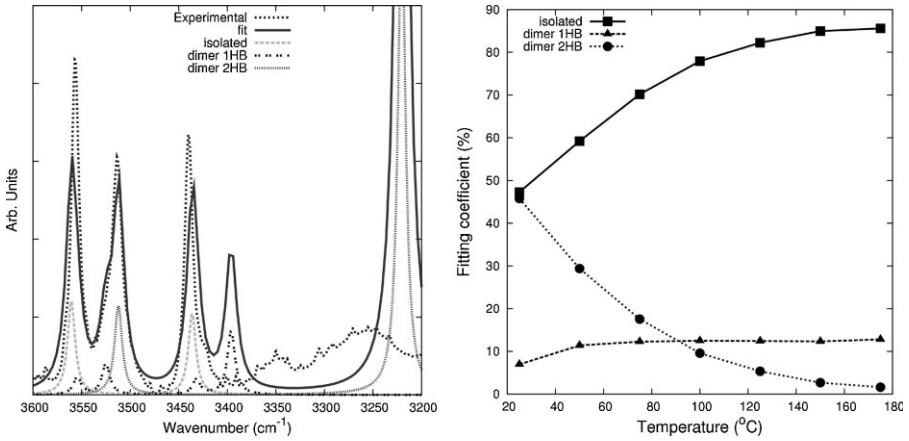

Figure 3.
Left: Fitting of IR spectrum recorded at 75 °C (see text for details). Right: Quantitative distribution of aggregates (associated to the isolated molecule and intermolecular complexes) as obtained by the fitting of the experimental spectra from 25 °C to 175 °C with the computed spectra.

H bond on neighbour atoms (the H of the nearby NH or the O belonging to the C=O) determines a modification of the electronic structure of the whole $-CONH_2$ groups, and then a change of the stretching force constants of the ''free'' NH bonds. The results reported in Table 1 show indeed how the stretching frequency of NH bonds is modulated due to these ''indirect'' effects of hydrogen bonding on ''free'' NH bonds belonging to H bonded dimers. In particular, this analysis allows to assign the experimental bands observed at 3560 cm^{-1} and 3438 cm^{-1} to the symmetric and antisymmetric NH stretchings of an isolated molecules (not involved in any H bond) while the band at 3512 cm^{-1} is assigned to NH stretching of ''free'' NH bonds of the dimer 2HB. The predicted frequencies of dimer 1HB (energetically less favoured with respect to dimer 2HB) can explains the appearance of shoulders in the experimental spectra as shown in the left panel of Figure 3 and in Table 1.

Based on this assignment it is immediate to give an interpretation of the trends observed when varying the concentration or temperature: since aggregation via H bonding is more favoured when increasing the concentration or decreasing the temperature then the band at 3512 cm^{-1} related to dimer 2HB should become more and more important for higher concentration or lower temperatures. These are indeed the trend observed in the experimental spectra reported in Figure 2.

The results of DFT calculations can be used also for a quantitative analysis of the temperature dependent IR spectra, as already done in Ref. [4] in the case of concentration dependent spectra: it is indeed possible to build a lorentzian fitting function as the weighted sum of the contributions of each molecular model. By the fitting of the experimental spectra at different temperatures in the ''free NH'' frequency range (3600–3400 cm^{-1}) the weight coefficients can be determined thus obtaining a quantitative description of the spectra in terms of the amount of the isolated molecules and dimers. In Figure 3 the fitting so obtained is shown for the IR spectrum at 75 °C and on the right the results of the fitting are reported for all the temperatures: it is immediate to verify that when increasing temperature the aggregation via H bonding is disfavoured, as demonstrated by the rapidly decreasing of the contribution of dimer 2HB and the increase of that of isolated molecules.

Based on this fitting, it is thus possible to give a quantitative interpretation of the experimental IR spectra in terms of interacting and isolated molecular species.

The previous analysis focused on the ''free NH'' stretching frequency region but further considerations can be done by inspection of the 3200–3400 cm^{-1} frequency range where the broad IR features due to ''H bonded'' NH stretching are observed. In the left panel of Figure 3, the experimental spectra in this range show two different broad bands: a main band is observed at 3247 cm^{-1} and it can be assigned to NH stretching modes of dimer 2HB; furthermore a band is also observed at 3350 cm^{-1} and it can be assigned to NH stretching modes of dimer 1HB. In both cases, the NH bonds are directly involved in H bonding. These assignements are explicitly reported in Table 1 and further support the reliability of our interpretation of the experimental IR spectra on DFT calculations.

Two Dimensional Correlation Spectroscopy

In the previous section we have shown that hydrogen bonds and molecular association phenomena give rise to specific spectroscopic markers (new bands) in vibrational spectra and changes in relative intensities and overall band shape. In order to follow by means of IR spectra the effects related to such interactions it is useful to study spectra evolution when a perturbation is induced in the system, as for example changing concentration or temperature. Such experiments are especially suitable to be studied by means of two dimensional correlation spectroscopy using the approach of generalized two dimensional correlation spectroscopy (2D COS)[9]. This approach has been recently used by us, while considering concentration changes as perturbation, in order to study the effect of specific chemical moieties on normal mode dynamics[10] of fluorinated systems. Moreover, temperature has been used as a perturbation useful to understand the chemistry of a cross-linking reaction[11]. In the present study we had the opportunity to study both concentration and temperature effects as revealed by 2D maps[1].

We considered the two characteristic regions of NH stretching and CO stretching, and the two different perturbations (concentration and temperature).

The synchronous 2D map, reported in Figure 4 show cross peaks at the following frequencies: 3560–3512 cm^{-1}, 3560–3438 cm^{-1}, 3560–3200 (broad) cm^{-1}, 3512–3438 cm^{-1}, 3512–3200 (broad) cm^{-1} and 3438–3200 (broad) cm^{-1}. As a general remark, peak intensities of the synchronous correlation map put in evidence the degree of coherence between two signals that are measured at the same time[12].

All cross peaks observed in the synchronous are related to the intensity changes of the different NH stretching components observed and assigned before; the signs of the cross peaks are all positive in agreement with the overall increasing of the amount of amidic groups with increasing concentration. As often happens in 2D COS, the asynchronous maps give us the most interesting information. As a matter of fact, cross peaks at (ν_i-ν_j) and their signs inform us about the temporal relationship of the IR signals associated to the normal modes at ν_i and ν_j.

Let us comment in detail the 2D asynchronous map (Figure 4) considering the cross peaks observed above the diagonal: 3560–3512 cm^{-1} (+) 3560–3200 cm^{-1} (broad) (+) 3512–3438 cm^{-1} (−) 3438–3200 cm^{-1} (broad) (+). Signs of these cross peaks are interpreted according to rules described in Ref. [9]: they are positive if the intensity change at ν_1 occurs predominantly before ν_2; they are negative if the change occurs after ν_2. Following these rules, we can conclude that the 3560 cm^{-1} and

[1]Dynamical spectra constituting the data set used in getting the synchronous and asynchronous maps have been built up using IR spectral subtraction of solutions at different concentrations (temperature) using as a reference the corresponding PFPE matrixes; once subtraction have been performed a baseline correction has been performed and the set of data has been ordered according to increasing concentrations c_i (increasing temperatures T_i).

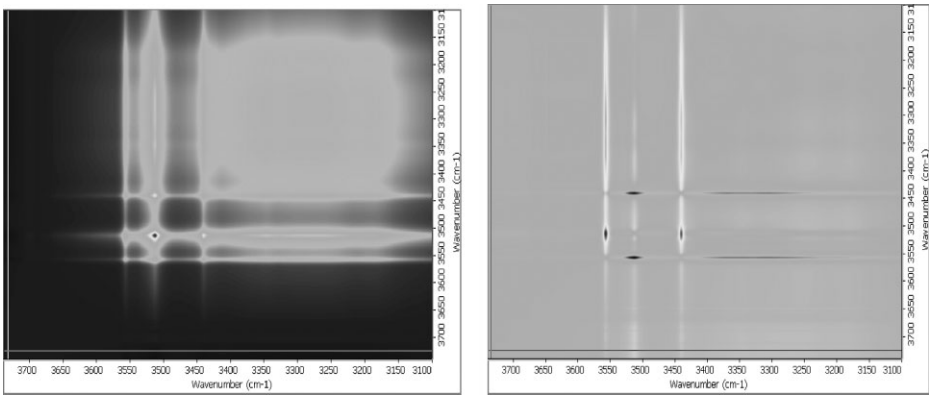

Figure 4.
Left: 2D Synchronous map: NH stretching region region at increasing concentration in FOMBLIN® M03. Peaks: 3560–3512 cm^{-1}; 3560–3438 cm^{-1}; 3560–3200 cm^{-1} (broad); 3512–3438 cm^{-1}; 3512–3200 cm^{-1} (broad); 3438–3200 cm^{-1} (broad) Right: Asynchronous map: NH stretching region at increasing concentration in FOMBLIN® M03: cross peaks at: 3560–3512 cm^{-1} (+); 3560–3200 cm^{-1} (broad) (+); 3512–3438 cm^{-1} (−); 3438–3200 cm^{-1} (broad) (+).

3438 cm^{-1} frequencies (assigned to antisymmetric and symmetric NH stretchings of the monomers, respectively) are related to lower concentration (first group of data in the set), while the 3512 cm^{-1} and 3200 cm^{-1} components (assigned to NH stretching of free and bonded NH belonging to molecules involved in H bonded complexes) are related to higher concentration (last group of data in the set).

The experiment at increasing temperature provide us with another independent set of data suitable for 2D COS; in Figure 5 the 2d synchronous map shows the same main features and cross peaks already observed in Figure 4. Interesting results have been obtained with the asynchronous map. As a matter of fact, cross peaks observed are: 3560–3512 cm^{-1} (−), 3560–3200 cm^{-1} (broad) (−), 3512–3438 cm^{-1}

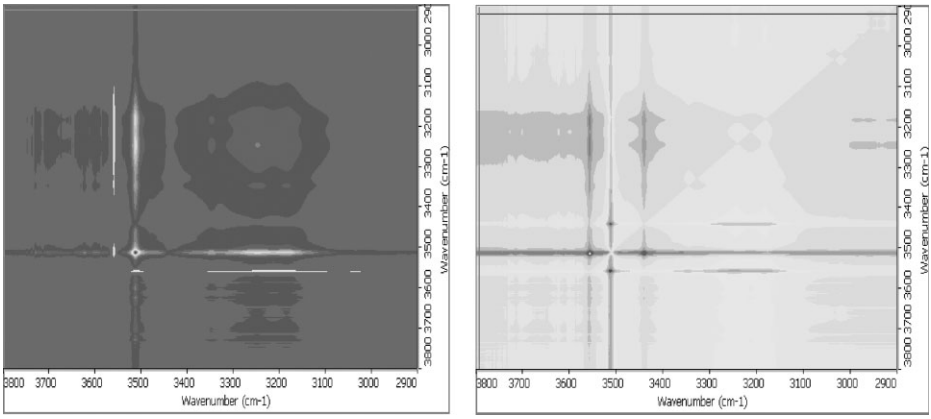

Figure 5.
Left: 2D Synchronous map: amide region in fomblin m03 at increasing temperature (RT-175 °C). Peaks: 3560–3512 cm^{-1}; 3560–3438 cm^{-1}; 3560–3200 cm^{-1} (broad); 3512–3438 cm^{-1}; 3512–3200 cm^{-1} (broad); 3438–3200 cm^{-1} (broad). Right: 2D Asynchronous map: amide region in FOMBLIN® m03 at increasing temperature (RT-175 °C) cross peaks at: 3560–3512 cm^{-1}(−); 3560–3200 cm^{-1} (broad)(−); 3512–3438 cm^{-1} (+); 3438–3200 cm^{-1} (broad) (−).

(+), 3438–3200 cm^{-1} (broad) (−). Frequencies and widths are similar to those observed in Figure 4 for the data set at different concentration, but in this case the signs of cross peaks are reversed. Accordingly, we can conclude that the components at 3560 cm^{-1} and 3438 cm^{-1} appears at higher temperature (namely at the end of the experiment), while the two components at 3512 cm^{-1} and 3200 cm^{-1} (broad and complex) appears at lower temperature (at the beginning of the experiment).

In Figure 6 we show the carbonyl region of IR spectra at different concentration and at different temperature. At least three components in can be identified: namely two higher frequency components (1776 and 1768 cm^{-1}) showing increasing intensity while the temperature is increased and one lower frequency (1758 cm^{-1}) showing the opposite behavior with temperature. A decrease of the concentration determines a similar evolution. Accordingly, the higher frequency component have been ascribed to free carbonyl bonds while the low frequency component to the carbonyl group acting as H bond acceptors in the dimers. 2D COS analysis has been carried out also in this region. It required careful pre-treatment of the data[13] included spectral subtractions and further baseline correction in the frequency region 1850 cm^{-1}–1680 cm^{-1}. In the case of the data while varying concentration this procedure is critical both regarding the choice of a reference intensity and signal to noise ratio, due to the very low IR signal at low concentration.

Indeed, the 2D asynchronous map (not shown here) built considering the concentration as perturbation does not show a clear correlation with features observed simply looking to the spectra of Figure 5. On the other hand, clear indications of the presence of the three already recognized different components is obtained looking to the synchronous map.

The arrows indicate the direction of increasing concentration/temperature.

Looking to the 2D maps relative to the experiment while varying temperature, the picture which can be derived is quite clear. The synchronous 2D map show two main regions: the first one with negative sign including cross peaks at 1776–1758 cm^{-1} and 1768–1758 cm^{-1}, while a region with positive sign at 1776–1768 cm^{-1}. The 2D asynchronous map shows a positive cross peak at 1776–1758 cm^{-1} (before 1758 cm^{-1}, then 1776 cm^{-1}), and another one at 1768–1758 cm^{-1}, positive but with very low correlation values. These features allow us to clearly assign the lower frequency component to the dimer 2HB componenent (which indeed is less populated as far the temperature increases, and the 1776 cm^{-1} to the monomer. As for the frequency at 1768 cm^{-1} the assignement is not so

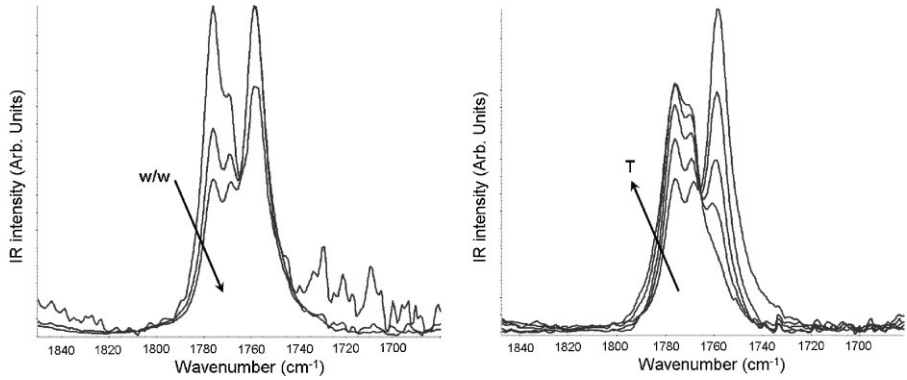

Figure 6.
Left: Carbonyl region: concentration 0,11%, 0,37%, 1,1% (the absorbance scale is not the same). Right: Temperature: 25–50–75–100–150 °C (same absorbance scale).

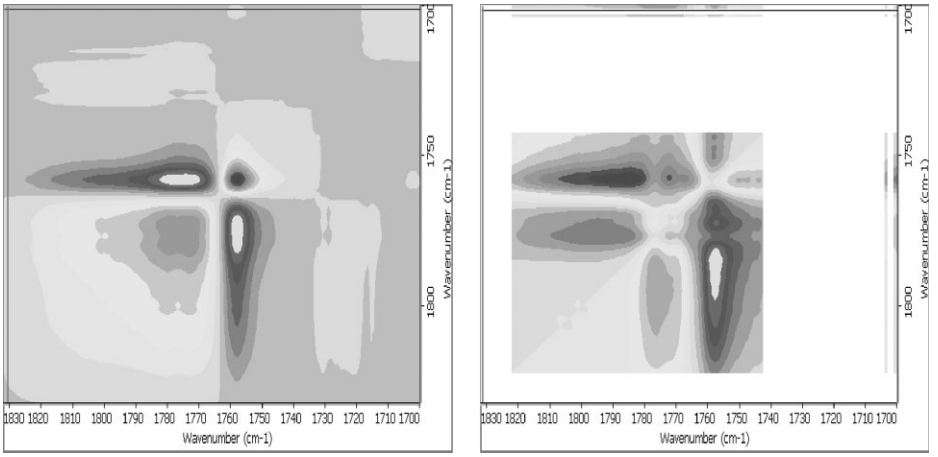

Figure 7.
2D synchronous (left) and asynchronous (right) data (CO region, increasing temperature as perturbation).

immediate: according to our calculations on models of dimers it should be assigned to the C=O stretching of a free C=O bond belonging to the dimer 1HB, which indeed is expected to present a temperature evolution not simply correlated to dimer 2H or to the monomer (see for instance Figure 3, right panel). In other words, the intensity ratio between the 1768 cm^{-1} and the 1776 cm^{-1} components evolves in a complex way because, by heating the sample, there is a wide range of temperatures where the population of both monomer and 1HB dimer increases at expense of the 2HB aggregates.

Conclusion

Infrared spectroscopy highlighted clear signals of the presence of different aggregates in fluorinated amides; DFT calculations allowed to specify the structure of the most probable aggregates, determining their relative contributions. By means of a fitting based on the computed values of frequencies and infrared intensities, the distribution of these aggregates has been determined in different temperature conditions.

The 2D COS approach applied to the experimental data sets as a function of both concentration and temperature confirmed the assignments and the evolution of the different components of bands in the frequency regions relative to NH stretching and CO stretching (3800–3100 cm^{-1}, 1850–1650 cm^{-1} respectively). The overall information obtained with 2D maps is similar for the two perturbations considered in the NH stretching region, with opposite trend due to increasing concentration and temperature. Some specific details have been detected by using the two different perturbations in the carbonyl region.

[1] S. Radice, G. Canil, P. Toniolo, P. A. Guarda, S. Petricci, A. Milani, M. Tommasini, C. Castiglioni, G. Zerbi, *Macromol. Symp.* **2008**, *265*, 218.
[2] P. Gavezotti, F. Riganti, in: "*Advanced Tribology and Applications*", CMC Publishing CO LTD, Tokyo 2007, p. 167–178.
[3] E. Mc Cafferty, in: "*Corrosion Control by Coatings*", J. H. Delinder, (Ed., Science Press, Princeton, N.J. 1979, 279.
[4] A. Milani, C. Castiglioni, E. Di Dedda, S. Radice, G. Canil, A. Di Meo, R. Picozzi, C. Tonelli, *Polymer*, **2010**, *51*, 2597.
[5] *Gaussian 03*, Revision C.02, M. J. Frisch, G. W. Trucks, H. B. Schlegel, G. E. Scuseria, M. A. Robb, J. R. Cheeseman, J. A. Montgomery, Jr., T. Vreven, K. N. Kudin, J. C. Burant, J. M. Millam, S. S. Iyengar, J. Tomasi, V. Barone, B. Mennucci, M. Cossi, G. Scalmani, N. Rega, G. A. Petersson, H. Nakatsuji,

M. Hada, M. Ehara, K. Toyota, R. Fukuda, J. Hasegawa, M. Ishida, T. Nakajima, Y. Honda, O. Kitao, H. Nakai, M. Klene, X. Li, J. E. Knox, H. P. Hratchian, J. B. Cross, V. Bakken, C. Adamo, J. Jaramillo, R. Gomperts, R. E. Stratmann, O. Yazyev, A. J. Austin, R. Cammi, C. Pomelli, J. W. Ochterski, P. Y. Ayala, K. Morokuma, G. A. Voth, P. Salvador, J. J. Dannenberg, V. G. Zakrzewski, S. Dapprich, A. D. Daniels, M. C. Strain, O. Farkas, D. K. Malick, A. D. Rabuck, K. Raghavachari, J. B. Foresman, J. V. Ortiz, Q. Cui, A. G. Baboul, S. Clifford, J. Cioslowski, B. B. Stefanov, G. Liu, A. Liashenko, P. Piskorz, I. Komaromi, R. L. Martin, D. J. Fox, T. Keith, M. A. Al-Laham, C. Y. Peng, A. Nanayakkara, M. Challacombe, P. M. W. Gill, B. Johnson, W. Chen, M. W. Wong, C. Gonzalez, J. A. Pople, Gaussian, Inc., Wallingford CT, 2004.

[6] A. D. J. Becke, *J. Chem. Phys.* **1993**, *98*, 5648.

[7] C. Lee, W. Yang, R. G. Parr, *Phys. Rev. B* **1988**, *37*, 785.

[8] G. C. Pimentel, A. L. McClellan, "*The hydrogen bond*", W. H. Freeman, San Francisco 1960.

[9] I. Noda, *Appl. Spectrosc.*, **1993**, *47*, 1329. I. Noda, A. E. Dowrey, C. Marcott, G. M. Story, Y. Ozaki, *Appl. Spectrosc.* **2000**, *54*, 236A–248A.

[10] S. Radice, C. Castiglioni, M. Tommasini, *J. Mol. Struct.* **2010**, *974*, 73.

[11] S. Radice, S. Turri, M. Scicchitano, *Appl. Spectrosc.* **2004**, *58*, 535.

[12] I. Noda, *Appl. Spectrosc.* **1990**, *44*, 550. I. Noda, *Bull. Am. Phys. Soc.*, **1986**, *31*, 520.

[13] M. Czarnecki, *Appl. Spectrosc.*, **1999**, *52*, 1583. M. Czarnecki, *Appl. Spectrosc.*, **1999**, *53*, 1392.

